Journal of the Indian Society of Remote Sensing (August 2018) 46(8):1307–1322
https://doi.org/10.1007/s12524-018-0799-6

RESEARCH ARTICLE

Mapping Urban Growth and Its Relation to Seismic Hazards in Istanbul

Cihan Uysal[1] · Derya Maktav[1] · Christopher Small[2]

Received: 13 February 2017 / Accepted: 29 May 2018 / Published online: 23 July 2018

Abstract
In Istanbul, one of the most densely populated cities of Turkey, the population has grown rapidly over the last 30 years. In addition to being one of the rapidly flourishing cities in Europe, the city is positioned on the seismically active North Anatolian Fault (NAF). The form and rate of Istanbul's fast urban growth has serious implications for seismic hazards. There have been some studies to map lateral urban growth for the city but they do not give satisfactory information about vertical urban growth and seismic hazards. We use DMSP night lights and Landsat data to map changes in land cover-land use in and around the city since 1984, and determine relations of these changes with the NAF. Changes in land use and intensity of development are identified by changes in night light brightness while changes in land cover are identified by changes in land surface reflectance. Aggregate changes in reflectance are represented as changes in subpixel mixtures of the most functionally and spectrally distinct spectral endmembers of land cover. Using standardized global endmembers, SVD composite images were produced for 1984, 2000 and 2011 and fraction change (δSVD) maps were produced for the decadal intervals. The results show that most of the urban expansion has occurred near the NAF. This has serious implications for seismic hazards in the future if the progression of large earthquakes continues to move westward toward the city.

Keywords DMSP · Earthquake · North Anatolian Fault · Spectral mixture model · Urban growth

Introduction

The percentage of population in cities was about 25% in 1950 increasing to 43% in 1980 and to 76% in 2010 in Turkey (TurkStat 2014). There have been large cities, such as Istanbul, Ankara, Izmir, Bursa and Adana where urban changes are being experienced and which draw migrations (Maktav et al. 2005; Maktav and Erbek 2005). In 1980, 10% of Turkey's population was living in Istanbul (4,741,890) and then this increased to 18% by 2011 (13,624,240) (TurkStat 2014). Compared to the other cities in Turkey, Istanbul provides the best economic opportunities as it has more industrial and trade areas. Therefore, migrations to the city continues from the other regions of the country (Geymen and Baz 2008).

Istanbul is located very close to the NAF that is known as one of the foremost hazardous earthquake regions all over the world (Figs. 1 and 2). This fault system extends along northern Turkey for more than 1400 km from 41°E to 29°E and accommodates about 25 mm/year right-lateral slip between Eurasian and Anatolian plates (McHugh et al. 2014; McClusky et al. 2000; Straub et al. 1997). The NAF has been unusually active seismically since the 20th century and it has been rupturing in a sequence of large earthquakes from east to west, starting in 1939 (Barka 1996; Toksoz et al. 1979; Cormier et al. 2006; Fichtner et al. 2013). 1999 earthquakes at Izmit and Duzce (M = 7.4/7.2) are major destructive westernmost earthquakes which resulted in at least 17,000 deaths (according to the official reports) and losses of properties (Ambraseys and Jackson 2000; Ergintav et al. 2014). Especially, the majority of the strain accumulation is known to take place in the northern branch of the fault (NAF-North) (Kurt et al. 2013) which covers Gulf of Izmit and extends across the Marmara Sea. The Marmara Sea segment of the NAF-N,

✉ Derya Maktav
maktavd@itu.edu.tr

[1] Geomatics Engineering Dept., Istanbul Technical Univ. (ITU), 34469 Istanbul, Turkey

[2] Lamont-Doherty Earth Observatory (LDEO), Columbia Univ., New York 10964, USA

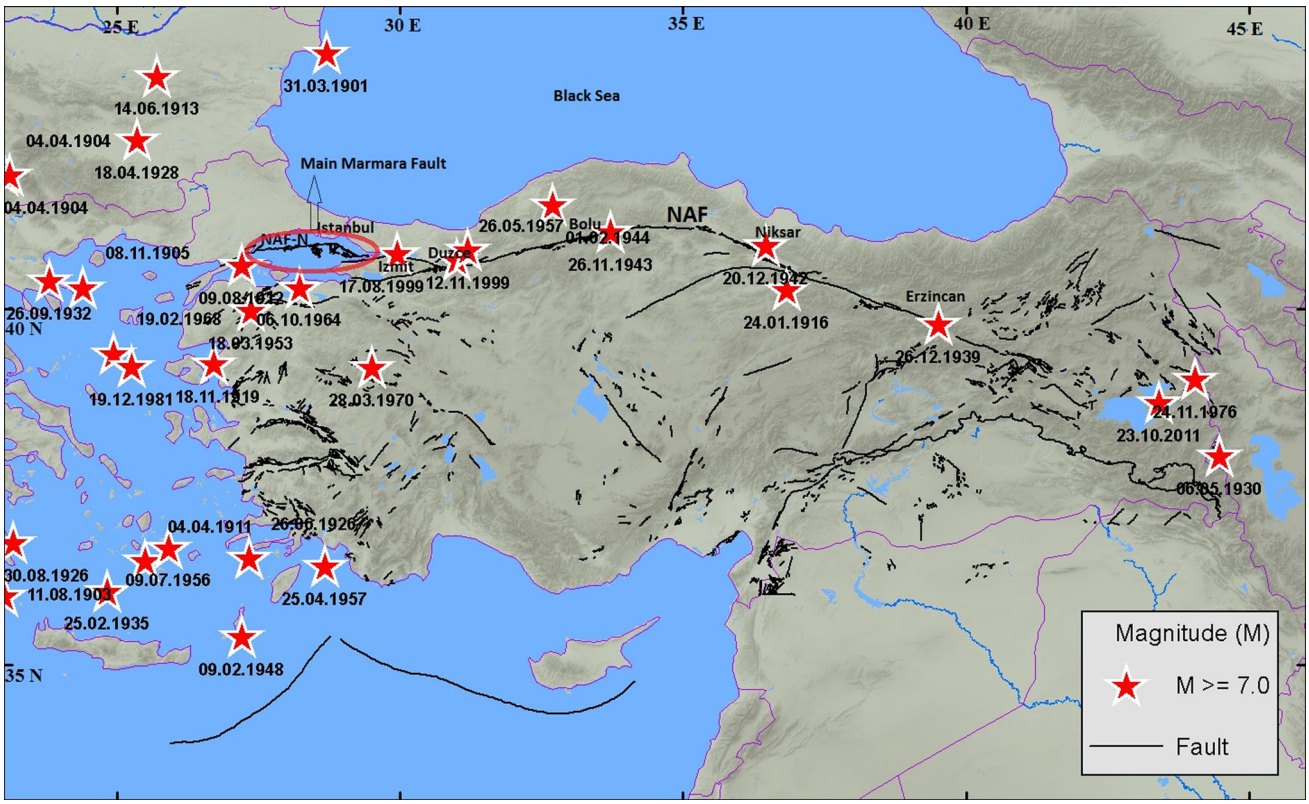

Fig. 1 The NAF system and historical earthquakes with M > 7 in Turkey. This figure shows destructive earthquakes (stars) and progression of seismicity from east to west on the NAF (KOERI 2015). The Main Marmara Fault, which currently has a 250 year seismic gap, is located south of Istanbul

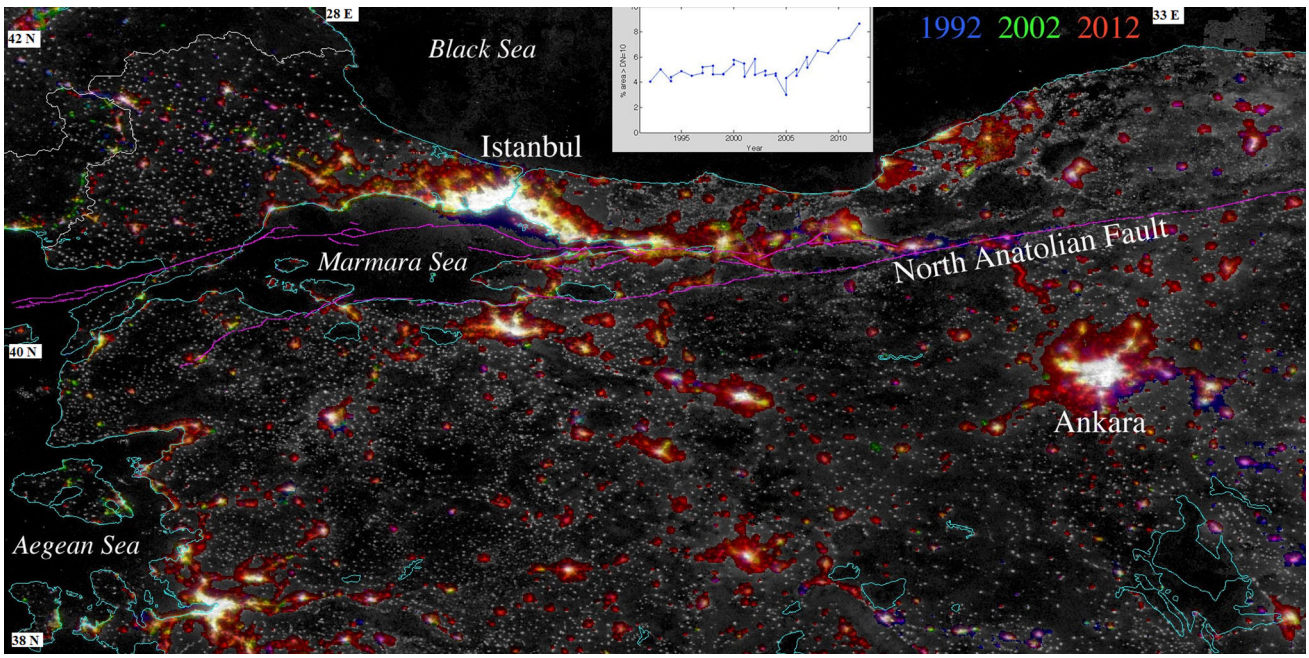

Fig. 2 Urban growth and lighted development along the North Anatolian Fault. Fused VIIRS + OLS night light image shows change in OLS night light between 1992 and 2012 as colors and 2013 VIIRS night light as gray shade. Warmer colors indicate brightening since 1992. While all large cities appear to have grown significantly, a band of development extending eastward along the fault from Istanbul is prominent. Inset plot shows doubling of lighted area post 2005 for all of Turkey

which covers Central Marmara and Princes' Islands Faults and it is known as the only remaining unruptured seismic gap (Ergintav et al. 2014; Ambraseys and Jackson 2000). The Princes' Islands Fault segment has seismic gap which has not been broken since 1766, while the northwest shore of the Marmara Sea stands out as unusually quiet over the last 500 years (Le Pichon et al. 2003; Armijo et al. 2005). Most observations and surveys including geologic, tectonic and historical evidences indicate that the city is exposed to considerable seismic risk. This probability of occurrence of an earthquake ($M > 7$) in Istanbul and vicinity has been estimated during the next 30 years as about 60% (Sengor et al. 2005; Parsons et al. 2000).

Existing maps of seismicity and soil properties allow mapping of seismic hazards but assessment of seismic risk requires additional information about vulnerability. A baseline assessment of vulnerability requires accurate maps of the spatial distribution of human settlements relative to the seismic risk. It is necessary to map the rate, location and type of development with respect to the NAF in order to assess this risk.

It is known that fast urbanization growth generally leads to issues like poorly planned infrastructure and unregulated development of hazard-prone areas. This kind of urbanization may lead to misuse and damage to cultivated areas, natural resources, such as water sources and green areas (Al-Rawashdeh and Saleh 2006). Urban growth and development have conventionally been mapped using discrete thematic classification techniques such as ISODATA and maximum likelihood. However, in such techniques, each pixel is matched single class value, which generally leads to low classification accuracy for the mixed pixels that represent most urban land cover (Shanmugam et al. 2006).

Although there have been some studies related to LCLU changes for Istanbul, only a few of them cover urbanization and do not give information about vertical urban growth or relate to seismic hazards. In Maktav and Erbek (2005) LCLU changes were analyzed using multitemporal satellite images (1984–1998 Landsat data) and supervised classification method in Buyukcekmece district of Istanbul. According to the results, urban growth has been caused by population migration into that area. Also, a decline of agricultural areas in different part of the region because of the rapid growth of settlement areas has been detected. Maktav and Sunar (2010) showed that land use for settlements between 1984 and 1998 increased by almost 20% in the Buyukcekmece district. Geymen and Baz (2008) conducted research focusing on the size and changes of built-up areas between 1990 and 2005 in Istanbul using Landsat images. The results showed that natural population growth in the city and intensive migration to the city have caused continuous urban growth. Moreover, industrialized areas were extended because of planned building and highway-to-sea connections. Jurgens et al. (2011) detected potential spaces available in Berlin, Ruhr area and Istanbul by adapting a main ruleset for object-based image analysis to QuickBird images. They also developed the GAUSmart tool which decides for the potential open areas concerning calculation of suitability maps for residential, industrial, agricultural and recreation areas. The study results showed that there were very limited spaces both for residential and industrial uses. There have been many studies related to urban land cover in the world. Recently, Henebry et al. (2015) described a novel method to monitoring urban land dynamics using the Multiple Indicators Detecting Significant Trends (MIDST) to process buildings in the megacities of America. They used a simple non-parametric trend analysis to a MODIS NBAR NDVI image time series of southeastern interior Brazil and determined changes in nearby lands influenced by urban dynamics.

The problem of spectral heterogeneity and inaccurate discrete classification can be resolved by using continuous field depictions of land cover like those provided by linear spectral mixture models (Gillespie et al. 1990; Adams et al. 1993). The spectral mixture analysis (SMA) was extensively applied to separate mixed pixels into its components. The consistency of the spectral mixing space for a variety of environments offers a simple three-component linear mixture model. This model may provide a consistent, general characterization of Landsat land surface reflectance and focused on SVD endmembers. When the spatial property of the mixing space is detected with endmembers chosen, it is forward to modify the linear mixture model for endmember fraction approximate calculations or estimates. The transposition of the linear mixing model for every image pixel gets fraction estimates for every endmember (Small 2004). In this model, the substrate endmember (S) matches a variety of rock, soil and impervious surfaces, the vegetation endmember (V) matches green vegetation and the dark surface endmember (D) matches water, shadow and nonreflective surfaces. Alterations in dark fraction have been associated with increasing deep shadow from both low rise and high rise vertical growth in São Paulo Brazil by Small et al. (2015).

The goal of the work is to provide a multi-sensor analysis of LCLU changes in the vicinity of the Istanbul conurbation in northeastern Turkey. We use a combination of night light and land surface reflectance to infer changes in land cover indicative of urban development and changes in land use. In contrast to previous studies, we attempt to circumvent the limitations of discrete classification of spectrally mixed urban land cover by mapping changes in reflectance as subpixel changes in mixtures of spectrally and functionally distinct endmember reflectances. We distinguish urban land cover as spectral mixtures of

impervious substrate and shadow (Small 2014) and map decadal changes with respect to the NAF. Also, measured GPS coordinates of the NAF are superimposed with fused VIIRS + DMSP/OLS image to compare urban growth acquired by spectral mixture analysis method.

Study Area and Data Used

As Istanbul is within the borders of Marmara Region in the northwest of Turkey, it has ~ 5343 km^2 of surface area. The Bosporus Strait, connecting the Black Sea to the Sea of Marmara separates Istanbul to two parts which are Europe (located on the west) and Asia (located on the east) (Fig. 3).

In the study, Landsat images, which have 30 m spatial resolution, from June 12, 1984 (TM), July 2, 2000 (ETM+) and June 23, 2011 (TM) were selected and used. All these data were processed as Level 1 terrain-corrected (L1T). They were usable in GeoTIFF format and they had UTM map projection with WGS84 datum. Also, L1T processing covers systematic geometric correction, radiometric correction, precision correction using ground control points, and the use of a digital elevation model (DEM) to correct parallax error due to local topographic relief. Moreover, DMSP/OLS acquired in 1992, 2002, 2012 and VIIRS images acquired in 2013 were used (Fig. 2). Fusing tri-temporal change images from annual composites of DMSP/OLS with more recent night light imagery from the VIIRS day night band (dnb) effectively reduces the extent of overglow while preserving brightness change information from previous decades of development (Small 2014). The higher spatial resolution and greater dynamic range and greater sensitivity of the VIIRS dnb allows it to detect smaller, dimmer lights than OLS without saturating in the bright urban cores (Small et al. 2013). In addition, the digitized NAF data (Emre et al. 2013) was used in Figs. 2 and 3. ENVI 4.8 software was used for exoatmospheric calibration and spectral unmixing.

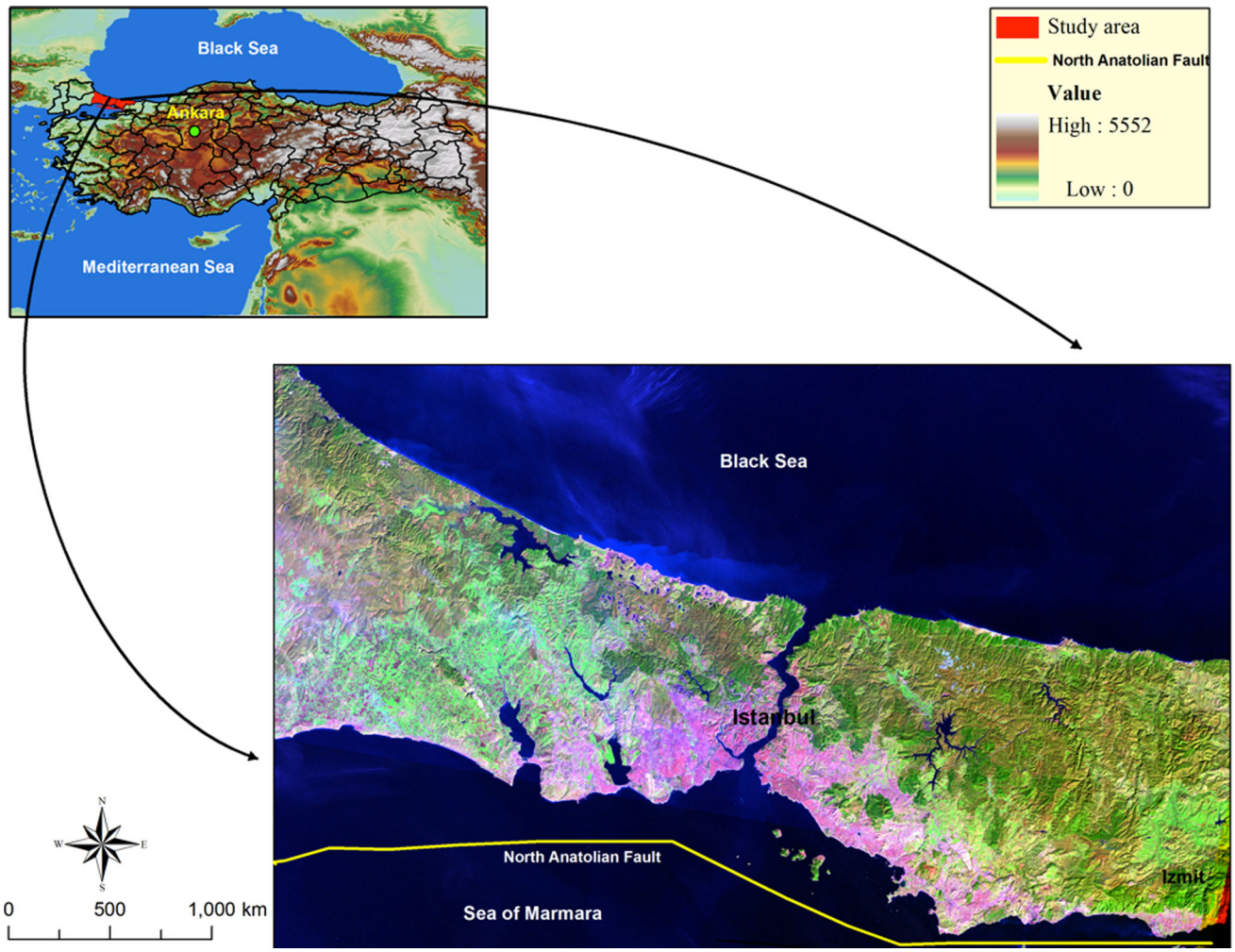

Fig. 3 The study area with the NAF

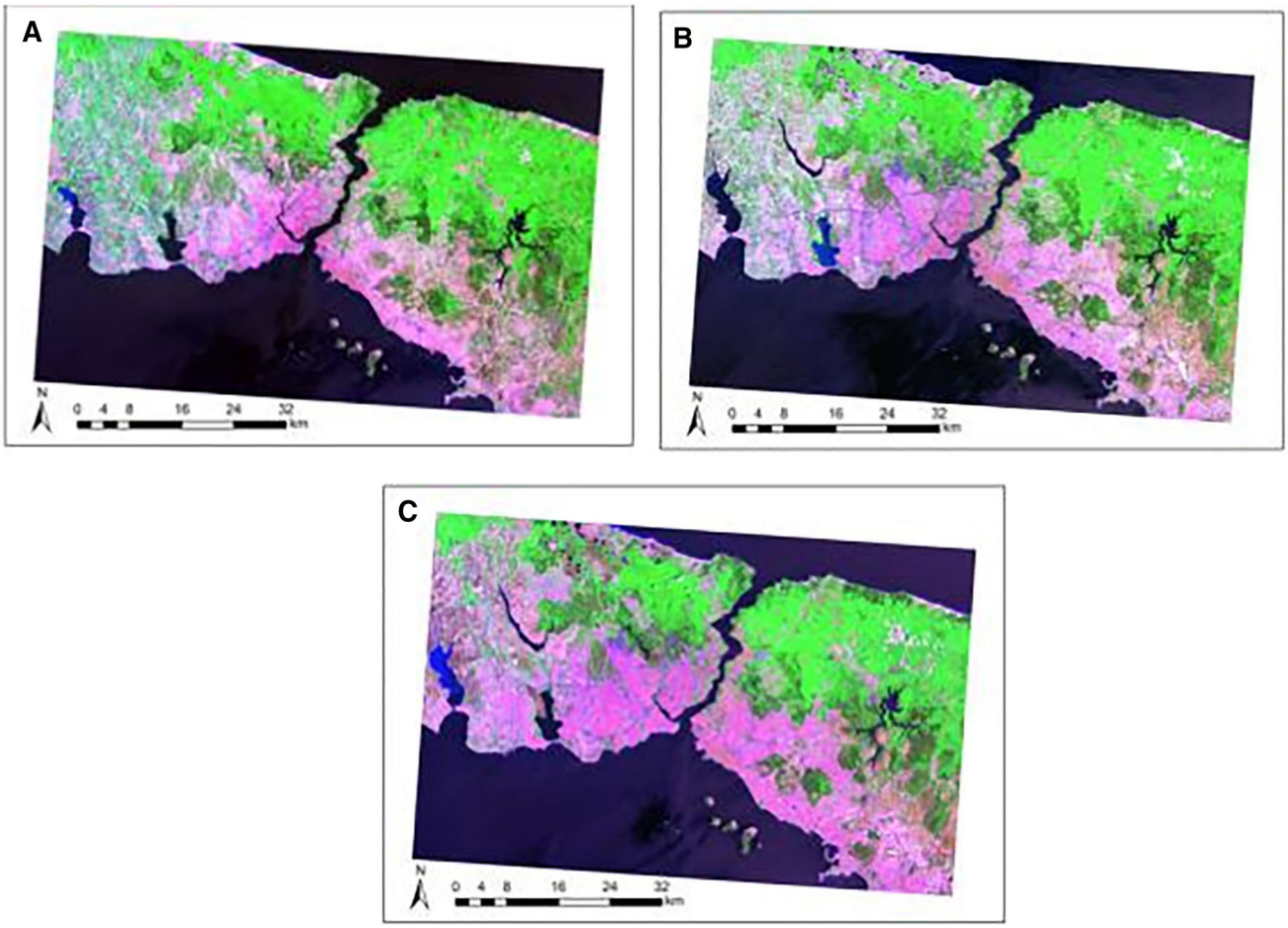

Fig. 4 Calibrated Landsat images **a** Landsat TM (12.06.1984), **b** Landsat ETM (02.07.2000), **c** Landsat ETM (23.06.2011)

Methodology

In this study, potential Landsat images were chosen and taken from USGS-Glovis (USGS-Glovis 2012). 1984, 2000 and 2011 Landsat images were chosen to analyze the regions prone to urbanization within the selected study area. The particular attention was also given to cloudless or cloud ratio which is $< 10\%$ while choosing these satellite data. The images collected under similar solar elevation conditions were used to reduce differences in illumination and shadow extent. Before applying the SMA method to the images, exoatmospheric calibration was adapted to the images. Normally, spectral radiance sensed by Landsat sensors is stored as 8 byte DN. But these values should be converted to radiance and then to top of atmosphere reflectance (ToA) values to minimize the changes arising from the sun-earth distance, solar geometry and spectral band gain differences.

A linear spectral mixture model was used to unmix the calibrated Landsat images. This mixing space topology may be represented precisely with the help of the standardized spectral endmembers (Small 2004). The endmembers employed in this research includes universal SVD endmembers obtained by the evaluation of images that can be applied for the worldwide research areas selected from different 100 geographical areas (Small and Milesi 2013). This globally representative mixing space has used a collection of 100 Landsat TM and ETM subscenes. PCA of the global composite indicates that 98% of the spectral variance can be represented within a 3D spectral mixing space. The mean SVD endmembers have defined a standard global mixture model for Landsat spectra (Small 2004). The standardized mixture models have provided consistency, rapid applicability and simplicity.

The SVD endmembers being used on an international scale and mixed pixels are given in percentage ratio and a linear spectral mixture model has been generated. δSVD maps were prepared as well by analyzing the distinctions of SVD layers acquired for different dates. The above mentioned maps are vital in reference to detecting the changes happening in LCLU for long time intervals. Moreover, the analyses have been carried out employing the Substrate layers from three chosen years determined particularly for

the evaluation of alterations in urbanization. Finally, in order to validate the SMA results we used Google Earth images with high spatial resolution.

Results and Validation

Figure 4 shows Landsat false color images (7-4-2 as RGB). The global endmembers were used to apply SVD linear mixture model and to obtain SVD maps (Fig. 5). δSVD maps created by taking differences of SVD values in different years indicate the changes in Substrate, Vegetation and Dark surface values (Fig. 6).

According to Figs. 5 and 6, Substrate areas expanded from 1984 to 2011 in areas consistent with the increasing spatial extent in night light brightness shown in Fig. 2. This expansion indicates that Istanbul's urban areas spread across the northern coastline of the Marmara Sea and the suburbs of Istanbul. The European side has more population than the Asian side and this caused more migrations as it has more trade regions and these migrations gained momentum in 1990s (Kaya and Curran 2006). Therefore, urban growth on the European side was greater than on the Asian side. Also LCLU changes were shown between 1984–2000 and 1984–2011, respectively (Fig. 6a–c). Rise in Substrate values is related to the newly built urban territories in the west of Istanbul is obviously noticeable. According to these maps, the fast increase in Substrate values between 1984 and 2000 has reduced in 2000 and in 2011 (Fig. 6b). The primary reason of this is related to the decline in the migration rate among rural regions between 2000 and 2011. According to TurkStat (2014), the rate of net migration to the city was 46% between 1995 and 2000. In the period of 2010–2011, this ratio decreased to 9%. It is also detected that the Dark surface value increased more between 2000 and 2011, S-D mixture is prevailing in central parts of Istanbul (Fig. 5). In this case, considering that Substrate value slightly decreased and Dark surface value increased in the built-up territories of the city, it is accordant with the ascent of shadow fraction in vertical urban increment. Shadow effect of the variable height of buildings has led to increase in Dark surface value. Since

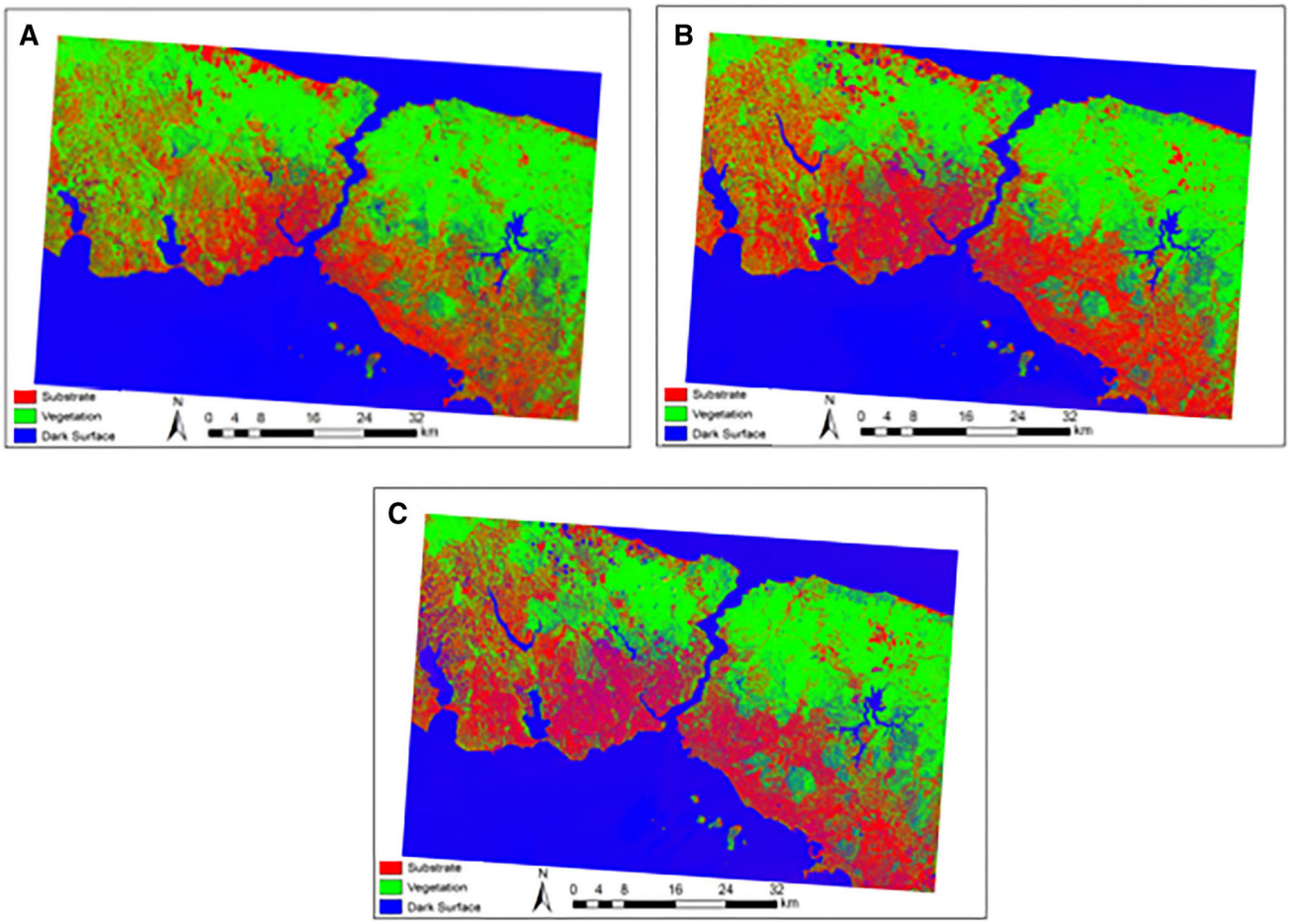

Fig. 5 SVD maps have been generated using the global endmembers and been shown as S, V and D fractions **a** SVD map (12.06.1984), **b** SVD map (02.07.2000), **c** SVD map (23.06.2011)

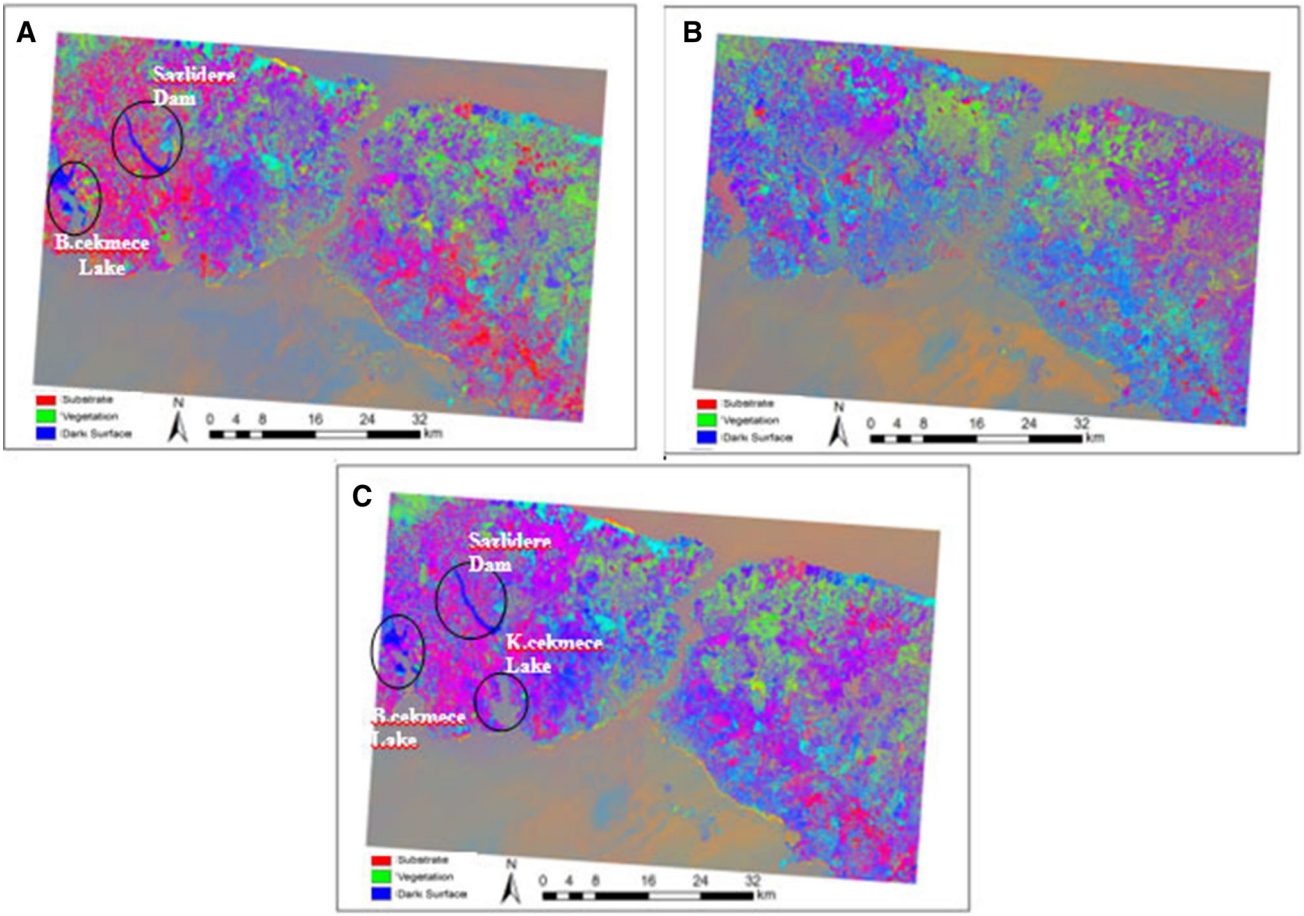

Fig. 6 δSVD maps **a** δSVD map between 1984 and 2000, **b** δSVD map between 2000 and 2011, **c** δSVD map between 1984 and 2011

2000, higher buildings have peaked especially in built-up regions and surroundings of Istanbul. These areas on both sides of the city were determined in Fig. 10 compared with high resolution Google Earth maps between 2002–2011 (Figs. 8 and 9). These maps have verified the results extracted from δSVD maps which show urban growth in both lateral and vertical scales.

The tri-temporal substrate map in Fig. 7 indicates substrate changes using the Substrate layers. According to the map, urban growth regions after 1984 are lying towards east and west of Istanbul across the coasts of Marmara Sea. These regions are characterized by hazardous seismic activity and they have very high risk for densely populated regions (Ambraseys and Jackson 2000; Fichtner et al. 2013). There is potential for an earthquake to directly affect this zone in the coming decades (Fichtner et al. 2013). Figure 2 indicates that the NAF and growing urban areas using night-time lights obtained by DMSP-OLS in 1992, 2002, 2012 and VIIRS in 2013. This figure indicates that night lights have brightened and multiplied since 1992; changes in SVD fraction suggest that the increases in night light brightness are associated with lateral and vertical growth of built area.

A significant increase in Substrate value was noticed in the territory around Kucukcekmece and Buyukcekmece Lakes on the tri-temporal substrate map. The areas with new urban growth, such as Esenyurt, Beylikduzu, Avcılar, Basaksehir, Kucukcekmece and Buyukcekmece located in this region were detected (Fig. 7). Ikitelli Industrial area in Basaksehir district in the northeast of Kucukcekmece Lake, the region between Kucukcekmece and Buyukcekmece lakes and region around which were opened to settlement played a significant role in the increase of this Substrate value (Maktav et al. 2000; Sunar 1998). In Fig. 7, the expanded part of Ataturk Airport which is to the east of Kucukcekmece Lake can be seen clearly. The Marmara Sea segment of the NAF-North includes Central Marmara Fault and Princes' Islands Fault. This segment is the only remaining unruptured seismic gap of the NAF-North and all these districts are close to it. According to the map, new urban growth regions are more than 190 km^2 on the European side.

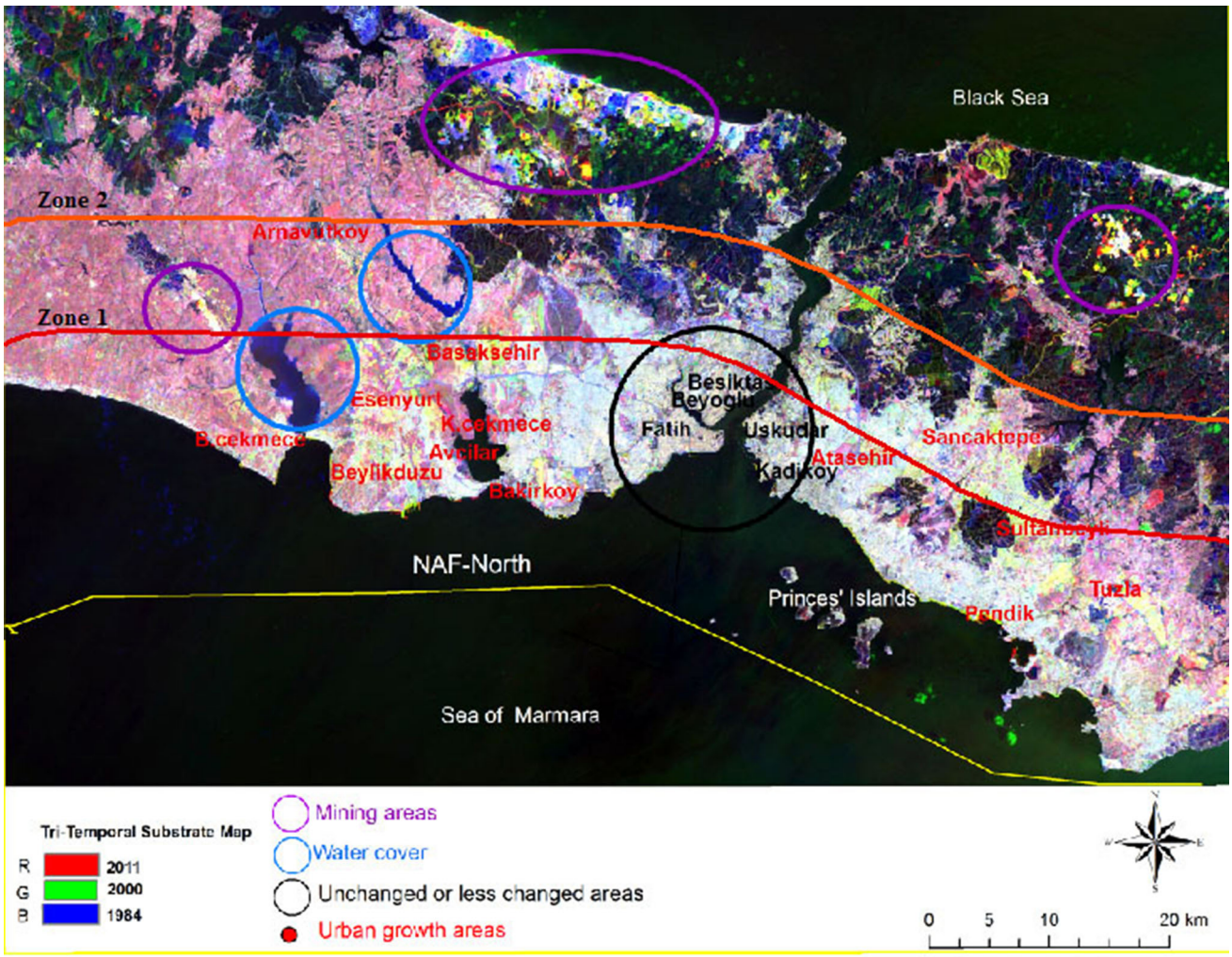

Fig. 7 Changed (color) and unchanged (gray) regions have been indicated on the tri-temporal substrate map using substrate values in 1984, 2000 and 2011

Table 1 Urban growth areas on both sides of Istanbul

Zones (Z)	Areas in European side (km^2)	Areas in Asian side (km^2)
Out of Z2	2	1
Z1–Z2	45	46
Z1	143	63
Total area	190	110

The districts on the north coast of the Marmara Sea and suburban districts like Esenyurt, Arnavutkoy and Basaksehir have high seismic hazards because most of them are very close to the NAF-North. During 1999 Izmit earthquake, damage was greater on the European side, although Avcilar and Buyukcekmece districts are located more than 90 km from the fault rupture. Hundreds of people died and it caused severe building damage (Ozmen 2000). The European side of the city was vulnerable to seismic hazards because of soil types and seismic wave amplification during 1999 Izmit earthquake (Dalgic et al. 2009; Ergin et al. 2004). In addition, regions closer to the northern coast of the Marmara Sea on European side of the city have thick filling material causing significant risk.

Sabiha Gokcen Airport, which is the second airport of the city, and the region developed around it can be seen on the tri-temporal substrate map (Fig. 7). The regions where the Substrate increase is the most on the Asian side are industry zones and settlement areas and the airport which was opened in 2001. Sultanbeyli, Sancaktepe, Atasehir,

Pendik and Tuzla are the districts where urban growth is experienced on the Asian side and urban growth areas are more than 110 km^2 on this side (Fig. 7). Most of these urban growth areas are close to Princes' Islands Fault (about 10–15 km) which is a part of the Marmara Sea segment of the NAF-North, therefore these districts have potential seismic hazards. Also, urban growth in Sancaktepe and Sultanbeyli districts, which are suburban areas, has continued towards the northern forest of the city.

The change in reflectance of the old city situated in the European side (Historical Peninsula) is extremely diminutive on the tri-temporal substrate map (Fig. 7).

In 1995, the region was also declared as a first degree archaeological, urban-archaeological, urban-historical protected area because there have been many buildings of historical value which remain unchanged in the above mentioned region (Dincer et al. 2011). Creation of new urban areas have been prevented in this region because of presence of intensive settlement and refusing new settlements for the protection of the historic fabric. Moreover, many regions that do not indicate a considerable alteration in Substrate value for years lie in central districts of Uskudar and Kadikoy in the Asian side and Beyoglu, Besiktas and Fatih in the European side (Fig. 7). The population density did not change considerably and even decreased in districts like Beyoglu and Fatih. There have been a lot of vulnerable old and historical buildings in these districts which may be damaged or collapsed during the next destructive earthquake in Istanbul (Erdik 2003).

It is detected that water covered areas were changed between 1984 and 2000. Viewing dark surface representation, transformations in Buyukcekmece Lake and Sazlidere Dam, which provide utility and potable water to Istanbul, were determined. Sazlidere Dam was built in 1996 and it is not detectable in both 1984 SVD and Landsat image. Consequently, while being represented primarily by Substrate and Vegetation values on the SVD map of 1984, this region is represented mainly by Dark surface value on the maps between 2000 and 2011. The dam area with 10 km^2 surface area may be regarded as the change area on 1984–2000 and 1984–2011 δSVD maps (Fig. 6a–c). Buyukcekmece Lake surface was enlarged because the dam was constructed on it in 1988. This change led to an increase in Dark surface value in this area (Fig. 6a–c).

Changes in reflectance also reveal increased mining activity in the vicinity of Istanbul. The rise in Substrate values in the mining area situated between the Black Sea and the Omerli Dam began in 1984 has continued after 2000 in the Asian side. Also, the change in mining regions spreading along the coastline of Black Sea in the European side is observable on the SVD maps. These regions that are mostly represented by Substrate value on Fig. 5a are expressed in Substrate and Dark surface values between 2000 and 2011. This is triggered by the water filling in gaps on the soil which took place because of mine activities. Therefore, Substrate value decreased in all around the most active mining areas in this territory and they are replaced in Dark surface values. The northern and northeastern areas of Arnavutkoy, employed as mining areas and quarries, and in the regions in Durusu, Akpinar, Yenikoy, Ciftalan and Kumkoy which are situated parallelly to the coastline of the Black Sea; some man-made ponds of variable sizes are located. Figure 7 indicates new mining fields and that Substrate value has increased on these areas. Also, Fig. 7 indicates quarries opened in the northwestern part of Buyukcekmece as substrate area. In addition, this substrate area is not linked to urban growth because interannual alterations in agricultural phenology which led to increase in substrate values of fallow agricultural fields.

Buffer analysis which is a basic spatial operation was built on the tri-temporal substrate map and two zones (Z1 and Z2) were acquired on the map (Fig. 7). While Z1 indicates 20 km distance from the NAF, Z2 indicates 30 km distance from the NAF. According to the analysis, most of urban growth regions on both sides of Istanbul have been in zone 1 (Table 1).

Vicarious Validation

While changes in substrate fraction are informative, they can also be related to changes in non-urban substrate such as fallow soils. For this reason, simultaneous changes in both substrate and shadow fractions were investigated. In the study δSVD maps were utilized to chart vertical urban growth within the city. In these areas, reflectance changed from substrate-dominant to substrate-dark mixtures, suggesting vertical growth with increasing shadow fraction. Using δSVD maps, new urban growth regions after 2000 Avcilar, Beylikduzu, Basaksehir, Arnavutkoy and Esenyurt were detected in the European side of Istanbul (Fig. 10a). High resolution images of 2002 and 2011 were employed in districts of Avcilar, Esenyurt and Basaksehir to check accuracy of the results. The test regions indicated that both results are strongly correlated and are verified using image pairs with high spatial resolution captured on 2002 and 2011 (Fig. 8). Similar comparison was applied to areas in the Asian side of Istanbul. Districts of Atasehir, Sancaktepe, Pendik, Umraniye, Tuzla and Cekmekoy were detected as urban growth regions (Fig. 10b). To test these results, high resolution image pairs were used for Pendik, Umraniye, Cekmekoy and Atasehir districts (Fig. 9). New urban areas built on the substrate areas were seen clearly in these maps and especially vertical growth in districts of Atasehir and Umraniye was seen on the maps.

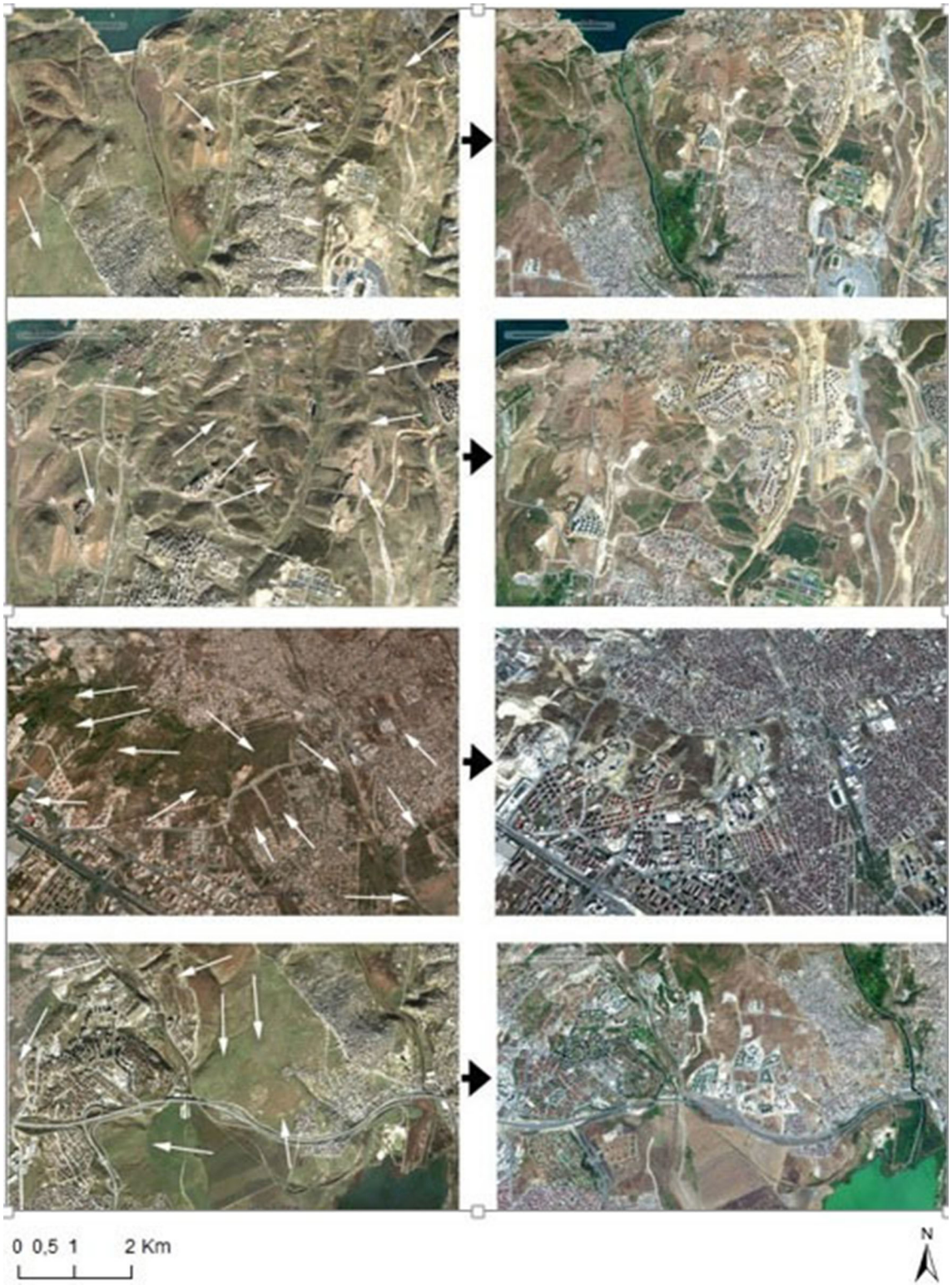

Fig. 8 High resolution images from Google Earth indicate urban rise between 2002 and 2011 in the European side of Istanbul (Google Earth 2015). Upper image pairs indicate urban rise in Basaksehir. Also, urban rise changes in Avcilar and Esenyurt districts are shown by the lower image pairs

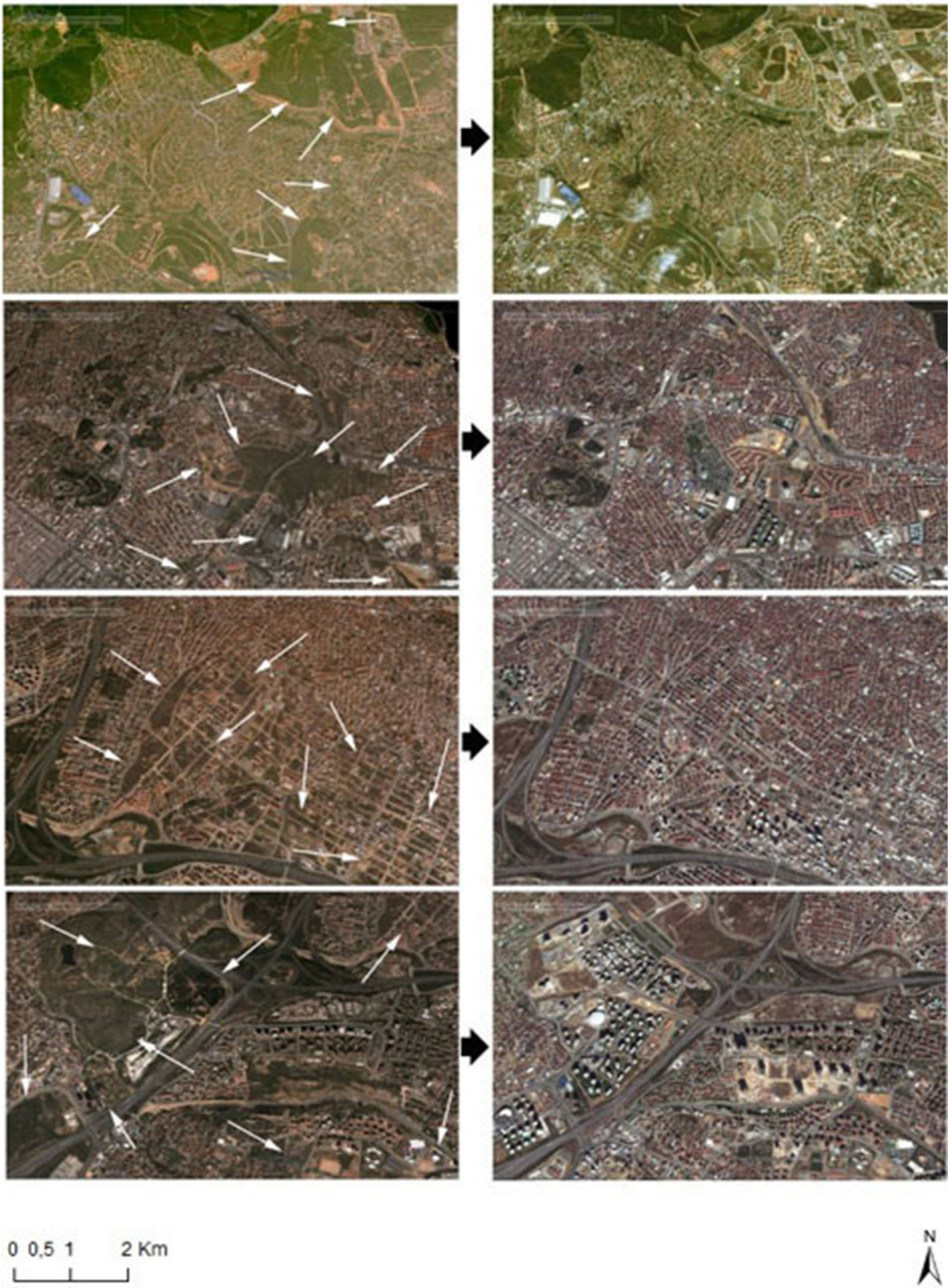

Fig. 9 The high resolution images from Google Earth indicate urban growth in 2002 and 2011 in the Asian side of Istanbul (Google Earth-2015). Urban growth in Pendik, Umraniye and Cekmekoy districts are shown in the upper image pair. Urban growth changes in Umraniye and Atasehir districts are shown in the lower image pairs

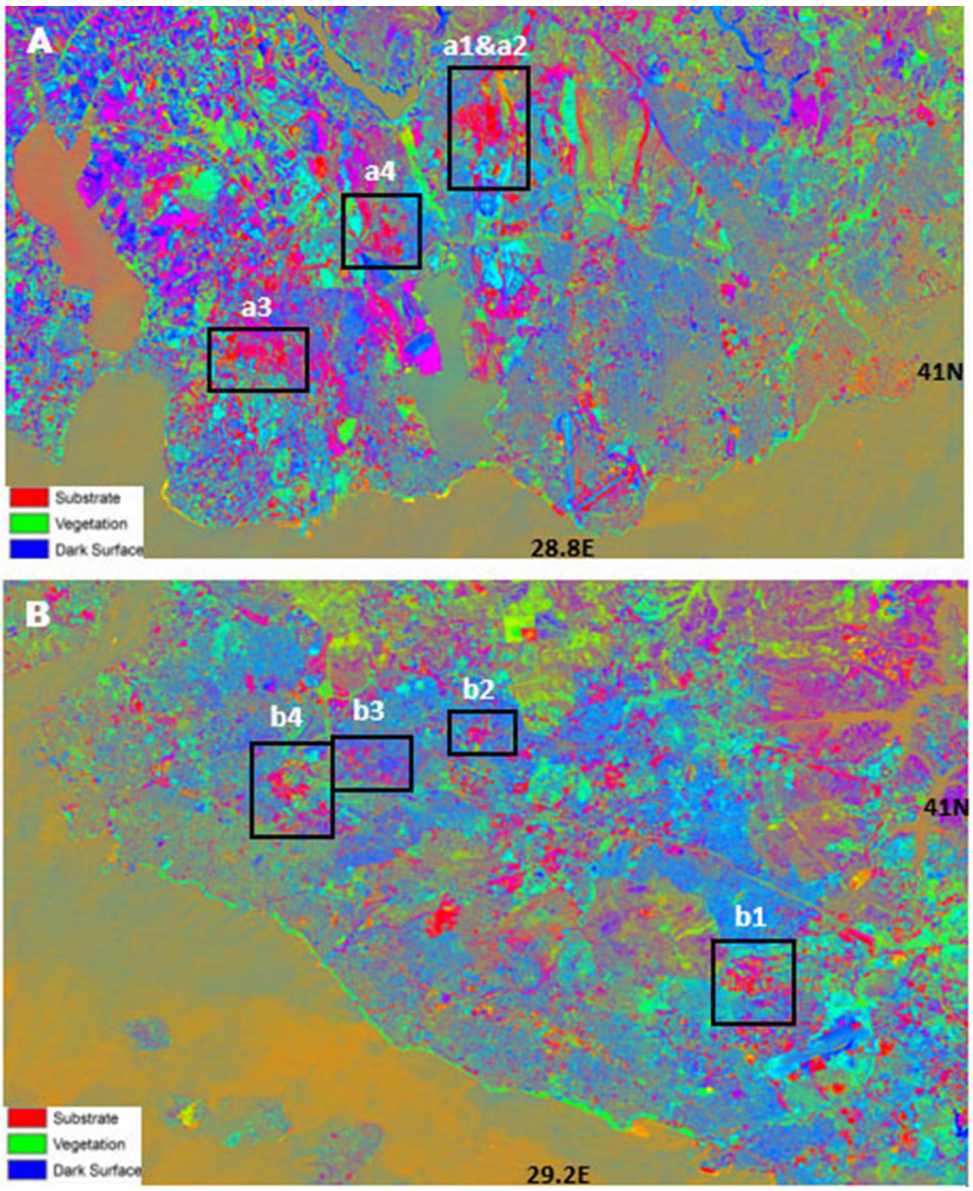

Fig. 10 The δSVD map indicates change regions where there have been evident increases in both Substrate and Dark surface fractions between 2000 and 2011 **a** European side, **b** Asian side

Accuracy assessment for urban growth regions in the city was applied in this reasearch. Using ArcMap 10.1 software, 50 random points were made up over the substrate fraction image (Fig. 11). Google Earth images with high spatial resolution, were used in the accuracy assessment as a reference map (Fig. 12). There had not been sufficient amount of high resolution images in 2000, hence, Google Earth images from 2001 were used to check new urban areas in the city. 45 points which represent urban area have matched in both substrate and reference maps and then accuracy assessment was measured as 90% for the urban test area. In addition, accuracy assessment for urban areas in the city was applied to DMSP/OLS images. These images have been compared to the reference map using same 50 control points. Of these, 42 points have been matched correctly and then accuracy assessment was determined as 84% for urban area acquired from DMSP/OLS images (Fig. 13).

Discussion

Decadal increases in night light brightness suggest considerable development around the periphery of Istanbul and eastward as far as Duzce along the NAF. Comparison of night light change images with multitemporal Landsat shows increases in dark fraction in substrate-dominated areas consistent with vertical growth causing increased building shadow in areas dominated by impervious substrates. Validation with high spatial resolution satellite

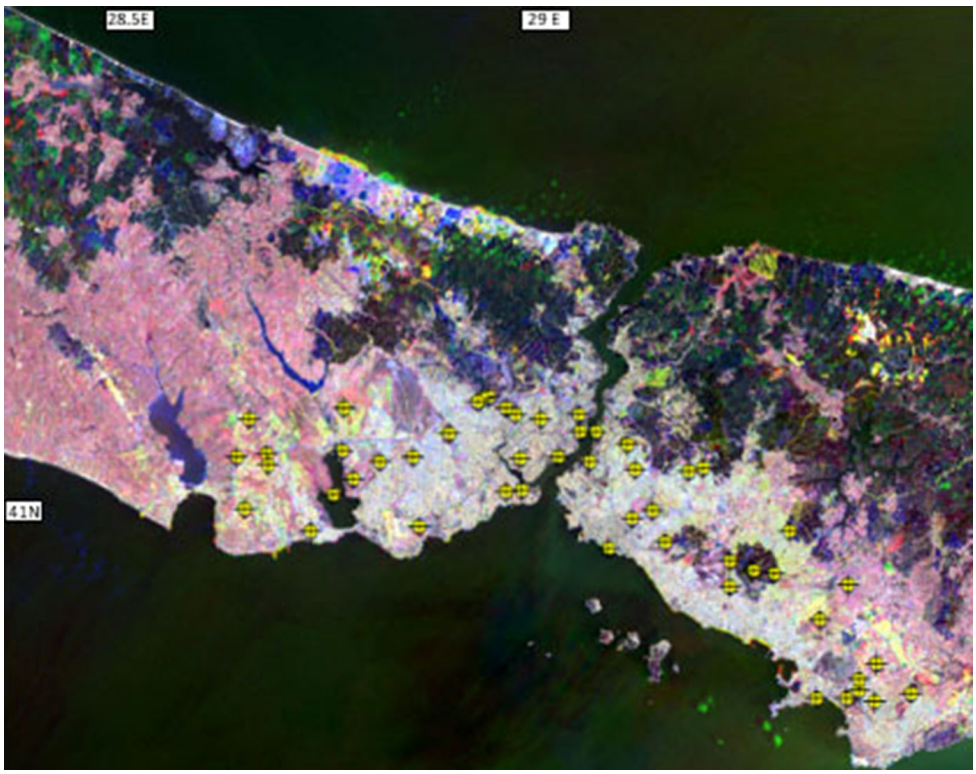

Fig. 11 The result map showing urban change areas (substrate map)

Fig. 12 The reference map (Google Earth -2015)

imagery verifies that the increases in dark fraction do correspond to shadows from new buildings in every validation site for which this imagery is available.

The conspicuous increase in night light brightness post-2005 (Fig. 2) is consistent with statistical evidence of national scale economic growth during this time. According to TurkStat (2015), the number of industrial enterprises increased from 17,559 (2005) to 24,400 (2011) and production value was doubled between these years. In parallel with this economic growth, electricity consumption

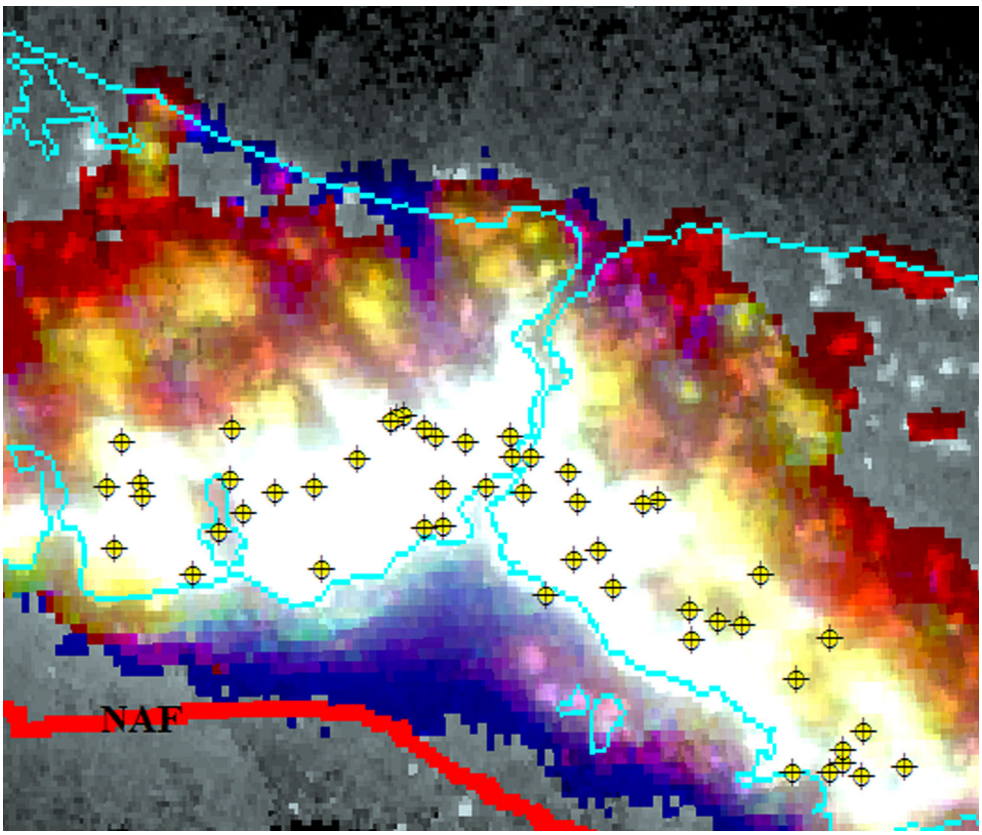

Fig. 13 DMSP-OLS images

increased by 78% from 132 BkWh to 235 BkWh between 2003 and 2013. Moreover, the number of registered new buildings and additions with construction permit increased from 50,140 (2003), to 114,254 (2005) and 121,266 (2013). After the 1999 Izmit earthquake and the economic crisis, there was a recession in the real estate sector until 2004. However, the real estate sector has boomed since 2005 as the economic development, affordable housing loans, increase in housing demand, and planned mass housing projects have led to the growth of the construction sector (Sur 2012). Given this rate of growth, it is not surprising that the extent and brightness of night lights has increased. However, the largest areas and greatest changes have occurred around Istanbul and eastward along the NAF.

The rapid rate of increase in urban development along the NAF has likely increased the overall seismic risk by increasing the exposure and vulnerability of an increasing number of people and amount of property in proximity to the fault. The fact that many of these areas are associated with increased shadow fraction suggests that some of the development occurs in the form of multi-story buildings with aspect ratios sufficient to create persistent deep shadow between buildings. In the absence of detailed maps of new construction, decadal change maps derived from night lights and Landsat, validated with higher resolution imagery, could provide spatially explicit inputs to updated regional scale seismic risk assessments.

The expansion of the city and other urban areas to the east has occurred along the North Anatolian Fault. This has serious indications for seismic hazard in the future if the progression of large earthquakes continues to move westward toward Istanbul. Especially, districts on the coasts of the Marmara Sea have become a more populous area of the city and earthquake risk has increased in this region after the 1999 earthquakes at Izmit and Duzce in western Turkey.

Conclusions

SMA was found to be a proper approach to detect the changes in land use in other cities applying the global endmember values, thanks to the rapid applicability provided by linear spectral mixture model. The results of the analysis indicate that it is possible to identify areas of potential urban development using increase in nighttime light brightness and to verify the presence of urban growth using changes in land surface reflectance consistent with increase in impervious substrate and building shadow. It is seen that Istanbul entered into a fast urban growth process

between 1984 and 2000, and after 2000 it continued as suburban areas in west–east direction across the coast of the Marmara Sea and the NAF.

Historical image pairs which have higher spatial resolution were obtained and used for vicarious validation of some areas showing magenta (increased S + D) post-2000 and they proved that increasing substrate and dark fractions suggest more than 190 and 110 km^2 urban growth regions in the Asian and European sides of the city respectively. One of the significant results of this reasearch is that urbanization has increased along the NAF. Urban development has increased in districts which were damaged by the Izmit earthquake in 1999 on the European side of Istanbul. This is significant because these densely populated areas have hazard-prone soil types and distances to the fault are very close-often less than 20 km.

Acknowledgements The authors express their gratitude to the Scientific Research Projects Department of the ITU, Scientific and Technological Research Council of Turkey (TUBITAK) for valuable support, and the Lamont-Doherty Earth Observatory (LDEO) of Columbia University for hosting the visit of Cihan Uysal.

References

Adams, J. B., Smith, M. O., & Gillespie, A. R. (1993). Imaging spectroscopy: Interpretation based on spectral mixture analysis. *Remote geochemical analysis elemental and mineralogical composition* (Vol. 7, pp. 145–166). New York: Cambridge University Press.

Al Rawashdeh, S., & Saleh, B. (2006). Satellite monitoring of urban spatial growth in the Amman area, Jordan. *Journal of Urban Planning and Development, 132,* 211–216. https://doi.org/10.1061/(ASCE)0733-9488(2006)132:4(211).

Ambraseys, N. N., & Jackson, J. A. (2000). Seismicity of the Sea of Marmara (Turkey) since 1500. *Geophysical Journal International*. https://doi.org/10.1046/j.1365-246X.2000.00137.x.

Armijo, R., Pondard, N., Meyer, B., Ucarkus, G., Mercier de Lepina, B., Malavieille, J., et al. (2005). Submarine fault scarps in the sea of Marmara pull-apart (North Anatolian Fault): Implications for seismic hazard in Istanbul. *Geochemistry, Geophysics, Geosystems*. https://doi.org/10.1029/2004GC000896.

Barka, A. (1996). Slip distribution along the North Anatolian Fault associated with the large earthquakes of the period 1939 to 1967. *Bulletin of the Seismological Society of America, 86,* 1238–1254.

Cormier, M. H., Seeber, L., Polonia, A., Cagatay, M. N., Emre, O., McHugh, C. M. G., et al. (2006). North Anatolian Fault in the Gulf of Izmit (Turkey): Rapid vertical motion in response to minor bends of a nonvertical continental transform. *Journal of Geophysical Research: Solid Earth*. https://doi.org/10.1029/2005JB003633.

Dalgic, S., Turgut, M., Kusku, I., Coskun, C., & Cosgun, T. (2009). The effect of soil and rock conditions on construction foundation on the European side of Istanbul. *Applied Earth Sciences, Kocaeli University, 2,* 47–70.

Dincer, I., Enlil, Z., Evren, Y., & Som, S. K. (2011). *Istanbul's historical and natural heritage values: Potential, risks and protection Issues* (pp. 74–75). Istanbul: Istanbul Bilgi University Publications.

Emre, O., Duman, T.Y., Ozalp, S., Elmaci, H., Olgun, S., & Saroglu, F. (2013). Active fault map of Turkey with an explanatory text 1:1250000 scale. General Directorate of Mineral Research and Exploration, *Special Publication Series, 30*, Ankara, Turkey.

Erdik, M. (2003). *Earthquake vulnerability of buildings and a mitigation strategy: Case of Istanbul*. Washington, DC: World Bank.

Ergin, M., Ozalaybey, S., Aktar, M., & Yalcin, M. N. (2004). Site amplification at avcilar, Istanbul. *Tectonophysics*. https://doi.org/10.1016/j.tecto.2004.07.021.

Ergintav, S., Reilinger, R. E., Cakmak, R., Floyd, M., Cakir, Z., Dogan, U., et al. (2014). Istanbul's earthquake hot spots: Geodetic constraints on strain accumulation along faults in the Marmara seismic gap. *Geophysical Research Letters*. https://doi.org/10.1002/2014GL060985.

Fichtner, A., Saygin, E., Taymaz, T., Cupillard, P., Capdeville, Y., & Trampert, J. (2013). The deep structure of the North Anatolian Fault Zone. *Earth and Planetary Science Letters*. https://doi.org/10.1016/j.epsl.2013.04.027.

Geymen, A., & Baz, I. (2008). Monitoring urban growth and detecting land-cover changes on the Istanbul metropolitan area. *Environmental Monitoring and Assessment*. https://doi.org/10.1007/s10661-007-9699-x.

Gillespie, A.R., Smith, M.O., Adams, J.B., Willis, S.C., Fischer, A.F., & Sabol, D.E. (1990). Interpretation of residual images: spectral mixture analysis of AVIRIS images. In *Anual JPL airborne visible/infrared imaging spectrometer (AVIRIS) Workshop*, pp. 243–290.

Google Earth 7.1.7.2606. (2002&2011). Asian side of Istanbul. 40°57′44.90″N, 29°14′11.91″E, DigitalGlobe 2015. https://www.google.com/earth/. September 23, 2015.

Google Earth 7.1.7.2606. (2002&2011). European side of Istanbul. 41°01′43.75″N, 28°44′36.45″E, DigitalGlobe 2015. https://www.google.com/earth/. September 24, 2015.

Google Earth 7.1.7.2606. (2001&2011). Istanbul. 41°03′57.62″N, 29°01′25.95″E, DigitalGlobe 2015-Terrametrics 2015. https://www.google.com/earth/. December 14, 2015.

Henebry, G., Zhang, X., Beurs, K., Kimball, J., & Small, C. (2015). Change in our MIDST: Toward detection and analysis of urban land dynamics in North and South America. In *JURSE-201,* Lousanne, Switzerland.

Jurgens, C., Siegmund, A., Maktav, D., Sunar, F., Esbah, H., Levent, T.B., Uysal, C., Kalkan, K., Mercan, O.Y., Akar, I., Thunig, H., & Wolf, N. (2011). Potential open space detection and decision support for urban planning by means of optical VHR satellite imagery. In *31. EARSeL symposium*, pp. 628–637, Prague, Czech Republic.

Kaya, S., & Curran, P. J. (2006). Monitoring urban growth on the European side of the Istanbul metropolitan area: A case study. *International Journal of Applied Earth Observation and Geoinformation, 8*(1), 18–25. https://doi.org/10.1016/j.jag.2005.05.002.

KOERI (Kandilli Observatory and Earthquake Research Institute). (2015). National Earthquake Monitoring Centre, Bogazici University, http://www.koeri.boun.edu.tr/sismo/indexeng.htm. Accessed 22 May 2015.

Kurt, H., Sorlien, C. C., Seeber, L., Steckler, M. S., Shillington, D. J., Cifci, G., et al. (2013). Steady late quaternary slip rate on the Cinarcik section of the North Anatolian fault near Istanbul, Turkey. *Geophysical Research Letters*. https://doi.org/10.1002/grl.50882.

Le Pichon, X., Chamot Rooke, N., Rangin, C., & Sengor, A. M. C. (2003). The North Anatolian fault in the Sea of Marmara. *Journal of Geophysical Research, 108,* B4. https://doi.org/10.1029/2002JB001862.

Maktav, D., & Erbek, F. S. (2005). Analysis of urban growth using multi-temporal satellite data in Istanbul, Turkey. *International Journal of Remote Sensing*. https://doi.org/10.1080/01431160512331316784.

Maktav, D., Erbek, F. S., & Jurgens, C. (2005). Remote sensing of urban areas. *International Journal of Remote Sensing*. https://doi.org/10.1080/01431160512331316469.

Maktav, D., & Sunar, F. (2010). Remote sensing of urban land use change in developing countries: an example from Buyukcekmece, Istanbul, Turkey. *Remote Sensing of Urban and Suburban Areas*. https://doi.org/10.1007/978-1-4020-4385-7_15.

Maktav, D., Sunar, F., Taberner, M., & Akgun, H. (2000). *Monitoring urban expansion in the Buyukcekmece District of Istanbul using satellite data*. Amsterdam, Holland: ISPRS.

McClusky, S., Balassanian, S., Barka, A., Demir, C., Ergintav, S., Georgiev, I., et al. (2000). Global Positioning System constraints on plate kinematics and dynamics in the Eastern Mediterranean and Caucasus. *Journal of Geophysical Research*. https://doi.org/10.1029/1999JB900351.

McHugh, C. M. G., Braudy, N., Cagatay, M. N., Sorlien, C., Cormier, M. H., Seeber, L., et al. (2014). Seafloor fault ruptures along the North Anatolia Fault in the Marmara Sea, Turkey: Link with the adjacent basin turbidite record. *Marine Geology, 353,* 65–83. https://doi.org/10.1016/j.margeo.2014.03.005.

Ozmen, B. (2000). Gulf of Izmit earthquake of 17 August 1999, damage condition, TDV/DR 010-53, Turkey Eartquake Foundation.

Parsons, T., Toda, S., Stein, R. S., Barka, A., & Dieterich, J. H. (2000). Heightened odds of large earthquakes near Istanbul: An interaction-based probability calculation. *Science, 288*(5466), 661–665. https://doi.org/10.1126/science.288.5466.661.

Sengor, A. M. C., Tuysuz, O., Imren, C., Sakinc, M., Eyidogan, H., Gorur, G., et al. (2005). The North Anatolian Fault: A new look. *Annual Review of Earth and Planetary Sciences, 33*(37), 112.

Shanmugam, P., Ahn, Y. H., & Sanjeevi, S. (2006). A comparison of the classification of wetland characteristics by linear spectral mixture modelling and traditional hard classifiers on multispectral remotely sensed imagery in Southern India. *Ecological Modelling, 194*(4), 379–394. https://doi.org/10.1016/j.ecolmodel.2005.10.033.

Small, C. (2004). The Landsat ETM + spectral mixing space. *Remote Sensing of Environment, 93*(1–2), 1–17. https://doi.org/10.1016/j.rse.2004.06.007.

Small, C. (2014). Mapping urban growth and development as continuous fields in space and time, Revista do Departamento de Geografia; Volume Especial CartoGeo, Revista do Departamento de Geografia da Faculdade de Filosofia, Letras e Ciências Humanas da Universidade de São Paulo - Brasil. https://doi.org/10.7154/rdg.2014.0114.0007.

Small, C., & Elvidge, C.D., & Baugh, K. (2013). Mapping urban structure and spatial connectivity with VIIRS and OLS night lights. In *IEEE proceedings of JURSE*-2013, Sau Paulo, Brasil.

Small, C., & Milesi, C. (2013). Multi-scale standardized spectral mixture models. *Remote Sensing of Environment, 136,* 442–454. https://doi.org/10.1016/j.rse.2013.05.024.

Small, C., Perez-Machado, R.P., Barrozo, L., & Luchiari, A. (2015). Mapping decades of urban growth and development using mutitemporal spectral mixture models, In: *Proceedings of XVII Symposio Brasiliero de Sensoriamento Remoto*, João Pessoa, PB, Brasil.

Straub, C., Kahle, H. G., & Schindler, C. (1997). GPS and geologic estimates of the tectonic activity in the Marmara Sea region, NW Anatolia. *Journal of Geophysical Research*. https://doi.org/10.1029/97JB02563.

Sunar, F. (1998). An analysis of changes in a multi-date data set: A case study in the Ikitelli area, Istanbul, Turkey. *International Journal of Remote Sensing*. https://doi.org/10.1080/014311698216215.

Sur, H. (2012). *Residential sector in Turkey. 5th Global Housing Finance Conference*. Washington DC: World Bank.

Toksoz, M. N., Shakal, A. F., & Michael, A. J. (1979). Space-time migration of earthquakes along the North Anatolian Fault Zone and seismic gaps. *Pure and Applied Geophysics PAGEOPH, 117,* 6. https://doi.org/10.1007/BF00876218.

TurkStat (Turkish Istatistical Institute). (2014). http://www.turkstat.gov.tr/UstMenu.do?metod=temelist. Accessed 25 June 2014.

TurkStat (Turkish Istatistical Institute). (2015). http://www.turkstat.gov.tr/PreTablo.do?alt_id=1055. Accessed 21 May 2015.

USGS Global Visualization Viewer. (2012). http://glovis.usgs.gov/. Accessed 2-12 September 2012.